New sulfonated pyrrole and pyrrole 3-carboxylic acid copolymers membranes via track-etched templates

M.-C. Clochard, C. Baudin, N. Betz, A. Le Moël, C. Bittencourt, L. Houssiau,
J.-J. Pireaux, Daniel Caldemaison

New sulfonated pyrrole and pyrrole 3-carboxylic acid copolymers membranes *via* track-etched templates

M-C. Clochard[1], C. baudin[1], N. Betz[1], A. Le Moël[1†]

C. Bittencourt[2], L.Houssiau[2], J-J. Pireaux[2]

Daniel Caldemaison[3]

[1]CEA-Saclay, DSM/DRECAM/LSI/LPI-Bat.466, F-91191 Gif-sur-Yvette Cédex, France

[2]LISE, FUNDP, 61 Rue de Bruxelles, B-5000 Namur, Belgium

[3]LMS, Ecole Polytechnique, Route de Saclay, F-91128 Palaiseau Cédex, France

KEY WORDS : polypyrrole, track-etched membrane, swift heavy ions, diaphragmatic method, sulfonation

[†] Corresponding author. Tel: +33-1-69-08-54-85; fax: +33-1-69-08-64-62 E-mail address : lemoel@drecam.cea.fr

ABSTRACT: New copolymers of polypyrrole and poly(3-carboxylic acid pyrrole) have been synthesized *via* diaphragmatic method using track-etched polycarbonate matrix. The carboxylic acid presence permits to introduce new functionalities such as sulfonate groups. The resulted copolymer membranes with tubules microstructure has been characterized by Scanning Electron Microscopy, X-ray Photoelectron Spectroscopy, Time-of-flight Secondary Ion mass Spectrometry and FTIR. By SEM it was observed that ion-track trajectories present characteristic of crossing. FTIR, XPS and ToF-SIMS proved the attachment of the Taurin molecule to the membrane. The thermal stability study shows that the polypyrrole copolymer membranes have an exceptional stability; decomposition was not observed up to 900°C.

1. Introduction

Polypyrrole, PPy, is insoluble and infusible which restricts its processability. To overcome these restriction, Zhitariuk and co-workers[1] proposed an original way of designing PPy microstructured membranes using track-etched polymer matrix[2]. These membranes proved to be an important device in the field of ultra-filtration and synthetic membranes[3]. In recent years, PPy/Nafion composites have been the subject of numerous fundamental studies and investigations for a wide range of applications[4,5,6]. The combination of both the electronic conductivity of the pyrrole with the high ionic conductivity of Nafion provides some applications for PPy-rich composites in batteries[4], super capacitors, and fuel cells[5,6]. Nafion is a well-known membrane for Proton Exchange Membrane Fuel Cell (PEMFC). Nevertheless, its thermal capacity during engine cycles is limited and its mechanical property can be affected by the presence of solvents, water content and by cation substitutions[7]. Even in composite form, these drawbacks remain unsolved. If the ionic conductivity as well as the ion-exchange capacity of Nafion could be conferred to the polypyrrole these drawbacks could be overcome. PPy microstructured membranes from track-etched membranes would enhance ion-exchange capacity. In combining PPy microstructured membrane technology with chemical functionalisation, the result would lead to a membrane which suits all the criterions required for an improved PEMFC.

The aim of this paper is then to report the synthesis of sulfonated PPy and PPy derivatives copolymers by oxidative polymerisation using track-etched templates. In fact, a substantial effect on the ionic conductivity has been already observed upon the incorporation of SO_3^- groups in the PPy polymeric chain[8].

2. Experimental Section

PC track-etched membranes were purchased from Waters. Pyrrole (Py) (Aldrich Chemicals) was distilled in vacuum and stored at ≤4°C in darkness prior to use. All the other reactants were used as received: Pyrrole 3-carboxylic acid (PyCOOH) (Acrôs), *para*-toluene sulfonic acid (*p*-TSA) (Aldrich), ferric chloride hexahydrate (FeCl$_3$:6H$_2$O), sodium hydroxide (NaOH), Taurin C$_2$H$_7$O$_3$NS (Aldrich), ethyl-3-(3-dimethylamino-propyl)carbodiimide C$_8$H$_{17}$N$_3$.HCl (EDC) (Fluka-Aldrich). These solvents were analytical grade. Deionized water was used.

Py and PyCOOH copolymerisation onto PC track-etched membranes (Waters) were performed using the diaphragmatic method described by Zhitariuk et al.[1,9]. The two-compartment cell was separated by the PC track-etched membrane. One compartment was filled with 10 ml solution (EtOH:H$_2$O) (50:50) of Py (0.15 N), PyCOOH (0.15 N) and p-TSA (0.1 N) as doping agent. The other one was filled with FeCl$_3$ solution (0.9 N) as an oxidant. The initial and the modified membranes were weighted to determine the weight of the final copolymer onto the matrix membranes. Dissolution of PC template membrane was then performed using NaOH 6N at 80°C for at least 2 h. The obtained dedoped black poly(Py-*co*-PyCOOH) membranes were washed twice in fresh water and 1 h in boiled water to remove any NaOH excess. The Poly(Py-*co*-PyCOOH) membranes were neutralized in acidic solution (1 N) for at least 2 hours before the Taurin immobilization. A coupling procedure was adopted and, after the last water washing, the clean membranes were allowed to react with EDC (10^{-2}M) and Taurin (3.2.10^{-2} M) for 24 hours in aqueous medium. The final membranes were washed again in fresh water and dried gently at room temperature.

Scanning Electron Microscopy (SEM). Scanning electron microscopy (SEM) was carried out with a Phillips apparatus equipped with a LaB$_6$ tip, and coupled with a PGT-Princeton

Gamma Tech. X-ray detector and a PRISM Digital spectrometer. The films and the cross-sections were coated with Au using a sputtering device before the analysis. Charge compensation with a low-energy electron flood-gun was necessary.

X-Ray Photo-electron Spectroscopy (XPS). X-ray photoelectron spectra were recorded on a HP5950A spectrometer using a monochromatic Al Kα X-ray source (1486.6 eV). The concentric hemispherical electron energy analyzer was equipped with a multichannel detector operating at a constant energy mode at an electron take-off angle of 51.5^{o}. Charging effects were neutralized using a flood gun operated at 2 eV kinetic energy. A pass energy of 150 eV was used for both survey and core level scans. The resolution was between 0.8-1 eV. Binding energies were determined by reference to the C_{1S} component due to aromatic carbons attributed as for poly(2-vinylpyridine) (P2VP) model[10] at 285.4 eV. Linear baseline for background subtraction and Gaussian functions were used for peak fitting. Atomic percentages were determined from peak areas by using Scofield factors[11] (C_{1S}=1, F_{1S}=4.43, O_{1S}=2.93, N_{1S}=1.8).

Time of Flight Secondary Ion Mass Spectrometry (ToF-SIMS). The mass spectra of the samples were recorded on a ToF-SIMS IV (ION-TOF GmbH) spectrometer. The secondary ions were generated by a pulsed gallium ion beam and extracted with a 2 keV voltage. Typical analysis conditions for this work were a 25 keV pulsed Ga^+ beam at a 45° incidence and a 2 pA pulsed current, rastered over a 130 μm $\times$ 130 μm area. The total ion fluency was kept below 3×10^{-12} ions/cm^2 to ensure static conditions. The mass resolution ($m/\Delta m$) near mass 29 was typically 8000.

Infrared Spectroscopy Measurements (FTIR). FTIR spectra of polymer membrane powders were recorded on a Nicolet Magna-IR™ 750 spectrometer equipped with a DTGS detector as a KBr pellet. Experiments were carried out cumulating 32 scans at a resolution of 2 cm^{-1}.

Thermogravimetry. The thermograms TG were recorded in air atmosphere at a heating rate of 20K/min using a thermal analyzer (Perkin Elmer DS1410D/9928J/DAD012).

2. Results and Discussion

Polymerisation and copolymerisation kinetics onto track-etched matrix

Elaborations of copolymer membranes were performed using the diaphragmatic method described by Zhitariuk et al. [1,9]. Polycarbonate microporous membranes were used as templates. The kinetics of the Pyrrole polymerisation and the copolymerisation of the pyrrole and pyrrole-3-carboxylic acid onto PC matrix (Figure 1) shows a rapid weight gain until 5 hours. Then an asymptotic variation leading to a conversion rate of 5 mol% at 24h is observed. This low conversion on the solid phase is due to the rapid diffusion of oxidant molecules and monomers through the PC matrix micropores resulting in a high conversion rate in the liquid phase. The available PC matrix area is also another parameter which limits the conversion. It is for this reason that we express the rate such as a grafting rate Q (wt%) instead of a conversion rate. Q is defined as follows:

$$Q = \frac{m_f - m_{PC}}{m_{PC}} \times 100 \qquad (1)$$

where m_f is the final weight of membrane obtained after polymerisation and m_{PC}, the initial weight of PC matrix.

As it is illustrated in Figure 1, a slight difference in polymerisation kinetic appears between the homopolymer PPy and the copolymer poly(Py-*co*-PyCOOH) at different temperature. In

fact, pyrrole is a very reactive monomer and is able to polymerize at low temperature (0°C).In contrast, pyrrole-3-carboxylic acid monomer needs a minimum of 50°C to polymerize properly. Nevertheless, when the copolymerisation occurs at 50°C, the polymerisation kinetic tends to be in the range of pyrrole homopolymerisation at 23°C.

Permeation study: a way to follow pore filling

To study our membranes, a simple cell with a free-standing membrane was used. Pressure was supplied by vacuum. Trans-membrane pressure (ΔP) was 10^4Pa. Ethanol permeation parameter L_m was calculated as follows:

$$L_m = \frac{J}{S_m.\Delta P} \tag{2}$$

where J - flow rate (m^3/s)

S_m – area of membrane surface (m^2)

Generally three parameters describe a membrane microstructure: pore diameter d_P, pore length l_P and porosity δ. They relate to macrocharacteristics of filtration by means of Hagen-Poiseuille equation:

$$J = \frac{\pi.d_P^4.\Delta P}{128.\eta.l_P} \tag{3}$$

where η represent the dynamic viscosity (Pa.s). This equation determines a laminar flow of liquid in one tube or pore with diameter d_P and length l_P. If we consider n pores on the membrane surface S_m, the equation 2 becomes:

$$L_m = \frac{n.J}{S_m.\Delta P} = \frac{n.\pi.d_P^4}{128.\eta.l_P} \tag{4}$$

therefore, $d_P = \sqrt[4]{\frac{L_m.l_P.128.\eta.S_m}{n.\pi}} = \sqrt[4]{\frac{L_m.l_P.128.\eta}{F.\pi}}$ $\tag{5}$

where F represents the fluency (number of ions per m^2 in considering one ion gives one pore).

We have performed multiple polymerisations of thirty minutes each. Between each polymerisation steps, we have permuted the monomer and oxidant compartments in order to get homogenous surfaces. Figure 2 displays the ethanol permeation values calculated from equation 4 between each polymerisation step of PPy and poly(Py-*co*-PyCOOH) membranes grafted onto PC matrix. When expressing the permeability in logarithm scale, a linear relationship is observed with the polymerisation time. Pyrrole and 3-carboxylic acid copolymer follows the same behaviour as polypyrrole but with a finer deposition at each polymerisation step leading to an enhanced permeability. Even if the polymerisation kinetics between the copolymer and the homopolymer is comparable at the studied temperatures, a difference in polymerisation kinetic subsists (Figure 1) and it can explain that finer copolymer deposition during pore filling. It may also come from a difference of structure density between the copolymer and the homopolymer.

By converting permeation data in equivalent diameter from equation 5, we observed that the polymer deposition inside the pores follows an exponential decay law (Figure 3). Different parameters coming from nanoscale intern pore diameter may govern that exponential decrease in polymer deposition such flow regime changes, electrostatic repulsions of polymer aromatic groups or diffusion limited molecules motion. Nevertheless, the simplest explanation would be that the pore diameter decrease implies a less important volume of penetrating available monomer solution inside pores. Consequently, the pore filling kinetic gradually diminishes and the polymer layer thickness reduces more and more step by step.

Final membrane microstructure

After the PC matrix dissolution under strongly basic conditions (NaOH 6N), SEM micrograph shows the final membrane structure (Figure 4a). From SEM pictures, we have observed a good correlation with equivalent pore diameter calculated previously from permeation measurements. In fact, the increase in the thickness of the pore wall after successive polymerisations can be easily followed (Figures 4b and 4c).

Figure 5 illustrates a cross-section of poly(Py-*co*-PyCOOH) membrane after PC matrix removal. The ion-track trajectories are not always in one direction as evidenced by the presence of multiple crosses formed by ions tracks copolymers replica. Some irradiations were done at +45° and others at -45° leading to microtubules cross-sections of 90°. This irradiation strategy is used to limit tracks overlapping. It could also be interesting to use this radiation procedure to increase the final mechanical properties of this kind of membranes.

Functionalisation of microstructured membranes: compositional verification

It is expected that the carboxylic acid groups of the copolymer membranes allow the anchor of Taurin molecules *via* common coupling reaction using water-soluble carbodiimide, EDC (scheme 1). The anchored Taurin molecules endow copolymer membranes with sulfonate functions. These sulfonate groups transfer protons and confer ion-exchange property to these new copolymer membranes.

In order to prove if Taurin immobilization was achieved chemical analysis were performed by XPS and ToF-SIMS. Figure 6 shows the negative ToF-SIMS spectrum recorded on the Taurin powder. This spectrum is characterized by a peak at $m/z = 124$ that is assigned to the Taurin molecular ion minus one hydrogen atom ($C_2H_7NO_3S^-$ or M - 1). Peaks appearing below m/z 124 give information about Taurin molecular fragmentation caused by ion impact during the ion emission process. The fragments at $m/z = 97$, $m/z = 80$, $m/z = 64$, $m/z = 48$ and $m/z = 32$ assigned to SO_4H^-, SO_3^-, SO_2^-, SO^- and S^- ions respectively, can be used to monitor

the Taurin immobilization as the sulphur atom is not a native element of the Poly(Py-*co*-PyCOOH) membrane. In fact, due to the use of the H_2SO_4 solution for neutralization of the Poly(Py-*co*-PyCOOH) membrane, traces of sulphur related fragments were found on the ToF-SIMS spectrum recorded on the membrane before the Taurin immobilization. However, on the spectrum recorded after the Taurin immobilization a low intensity peak related to the Taurin molecule appeared at *m/z* 124 (Figure 7) and the normalized intensity of the peaks related to the sulphur fragments increased; specifically marked was the increase of the sulfonate ion SO_3^- ion by a factor of 4.3. These suggest the presence of Taurin immobilized on the membrane. The low intensity of the Taurin molecule related peak can be associated to the fact that this molecule is strongly bond to the surface of the membrane and during the ion bombardment it is mainly fragmented.

Figure 8 displays the comparison of the C_{1S} XPS core level spectra recorded on Taurin substituted and non-substituted poly(Py-*co*-PyCOOH) membranes. Taurin substitution is evidenced by the peak width enlargement. Figure 9 (a) shows the C_{1S} core level spectrum recorded on the non-substituted poly(Py-*co*-PyCOOH) membrane, and the results of its fitting analysis. To reproduce the experimental data, four Gaussian functions and a linear background were used. Aromatic carbons (1) are attributed as for poly(2-vinylpyridine) (P2VP) model[10] at 285.4 eV. The shake up is fitted near 291 eV. The photoelectrons emitted from carbon atoms present in C-N PPy ring (2) and carboxylic acids (3) generated respectively the Gaussians at 286.2 eV and 289 eV. Figure 8 (b) displays the C1s core level spectrum recorded on Taurin substituted poly(Py-*co*-PyCOOH) membrane. To properly reproduce this data, apart from the four previously used Gaussians functions, two others were added to the fitting analysis. The new Gaussians functions were generated by photoelectrons emitted from carbon atoms in C-S groups (5) at 285.8 eV and from carbon atoms in amide groups (4) at 288.2 eV.

Comparing the results of the peak analysis, it was found that the area of the peak associated to carboxylic acid near 289 eV decreases from 11.2 % (theoretical value equals to11.1 %) to 5.7 % while the area of the C-N peak increases from 38.4 % up to 41.3 % and the area of the C=C peak decrease from 42.8 % to 27.3 %. The increase in the C-N peak area and the decrease of C=C peak area supports the assumption of Taurin immobilization. In fact, as shown on scheme 1, the chemical composition of the Taurin add a C-N bond conferring a theoretical 1.45 % increase of C-N content (2) and globally the C=C contribution (1) decreases theoretically from 44 % in carbon content for poly(PPy-*co*-PPyCOOH) to 36 % for poly(PPy-*co*-CONH-Taurin). Although a relatively good correlation, the variations observed from theoritical values show that the membranes surface chemical composition is slightly different from simple scheme model. The remaining 5.7 % carboxylic acid moieties suggests: i) the presence of PPy oxidation residue[12] and/or ii) a non-complete substitution which can be caused by a lack of accessibility of some carboxylic acid sites.

Figure 10 displays FTIR spectra of poly(Py-co-PyCOOH) and poly(Py-co-PyCONHTaurin). The bands at 1040 and 1107 cm^{-1} represent the symmetric and asymmetric streching vibration of the sulfonated group, respectively. It is important to note that the peak at 1700 cm^{-1} in spectrum (a) which corresponds to C=O vibration of the carboxylic acid decreased after Taurin attachment in favour to amide I peak arising at 1640 cm^{-1} and amide II peak at 1569 cm^{-1}.

Microstructured membranes thermal stability

Thermogravimetric analysis (TGA) permits to assess the thermal stability of each polymer membrane. As shown on figure 11, the data obtained for the dedoped polypyrrole synthesized in solution is similar to those obtained previously[13]. The TG of the polypyrrole powder shows only one major weight loss step at 475°C from derivative curve event. There is a small weight

loss of 8% below 100°C corresponding to water content. When polypyrrole has been synthesized by diaphragmatic method and the resulting PPy microstructured membrane was revealed by matrix dissolution, we observed an unexpected thermal behaviour. In fact, under thermal treatment, PPy membranes behave completely differently from PPy in solution showing no decomposition event, even when heating up to 900°C (Figure 11). This exceptional thermal stability is also observed for copolymer membranes. It is not affected by Taurin modification. Such a thermal stability on PPy derivatives has not yet been reported and it points out the great impact of the structure to the thermal behaviour. This is of great interest concerning PEMFC applications.

4. Conclusions

Copolymers of polypyrrole and poly(3-carboxylic acid pyrrole) have been successfully synthesized *via* diaphragmatic method using track-etched PC matrix. Permeation data permitted to obtain easily an equivalent pore diameter which has been confirmed by SEM. From permeation results, we could observe that polymer deposition layer on PC matrix was finer in case of copolymer compared to homopolymer of pyrrole. This difference was due to polymerisation kinetics variations. It might also come from a structural difference between the copolymer and the homopolymer leading to a denser layer in case of copolymer. After PC dissolution, poly(Py-*co*-PyCOOH) membranes with tubules microstructures were obtained. The tubules presented characteristic of crossing ion tracks. The resulting membrane with tubules microstructure should exhibit an enhanced ion-exchange capacity. The thermal stability of the membranes has shown no decomposition event up to 900°C, even after sulfonation by Taurin immobilization.

Sulfonation by coupling reaction with Taurin was verified by XPS, ToF-SIMS and FTIR. It suggests that other functionalities can be introduced using this protocol on such copolymer microstructured membranes opening a vast field of applications.

Acknowledgements

References

(1)   Zhitariuk, N. I.; Le Moël, A.; Memilliod, N.; Trautman, C. *nucl. instr. and meth.* **1995**, *105*, 204.

(2)   Spohr, R. *Ions Tracks and Microtechnology. Principles and Application.*; Friedr. Vieweg&Sohn Verlegsgschaft mbH: Braunschweig, 1990.

(3)   Demoustier-champagne, S.; Ferain, E.; Jérôme, C.; Jérôme, R.; Legras, R. *Eur. Polym. J.* **1998**, *12*, 1767-1774.

(4)   Blasiak, M.; Golimowski, J.; Maksymiuk, K. *Pol. J. Chem.* **2001**, *75*, 1719.

(5)   Langsdorf, L. L.; Sultan, J.; Pickup, P. G. *J. Phys. Chem. B* **2003**, *107*, 8412-8415.

(6)   Easton, E. B.; Langsdorf, B. L.; Hugues, J. A.; Sultan, J.; Qi, Z.; Kaufman, A.; Pickup, P. G. *Journal of The Electrochemical Society* **2003**, *150*, C735-C739.

(7)   Kawano, Y.; Wang, Y.; Palmer, R. A.; Aubuchon, S. R. *Polimeros: Ciencia e Tecnologia* **2002**, *12*, 96-101.

(8)   Sahin, Y.; Aydin, A.; Arslan Udum, Y.; Pekmez, K.; Yildiz, A. *Journal of Applied Polymer Science* **2004**, *93*, 526-533.

(9)   Ermolaev, S. V.; Jitariouk, N.; Le Moël, A. *Nuclear Instruments and Methods in Physics Research B* **2001**, *185*, 184-191.

(10)   Beamson, G.; Briggs, D. *high resolution XPS of organic polymers: the Scienta ESCA300 database*; John Wiley & Sons Ltd., 1992.

(11)   Scofield, J. H. *J. Electron Spectrosc. Relat. Phenom.* **1976**, *8*, 129.

(12)   De Giglio, E.; Losito, I.; Dagostino, F.; Sabbatini, L.; Zambonin, P. G.; Torrisi, A.; Licciardello, A. *Annali di Chimica* **2004**, *94*, 207-218.

(13)   Syed Abthagir, P.; Saraswathi, R. *Materials Chemistry and Physics* **2005**, *92*, 21-26.

Scheme 1. Taurin immobilization onto poly(PPy-co-PPyCOOH) membrane

Figure 1: Polymer mass variation onto PC matrix versus polymerisation time: PPy at 23°C (●), poly(Py-*co*-PyCOOH) at 50°C (○) .

Figure 2: Ethanol permeabilities of PPy (●) and poly(Py-*co*-PyCOOH) (○) membranes onto PC matrix at different polymerisation time

Figure 3: Equivalent pore diameters of PPy (●) and poly(Py-*co*-PyCOOH) (○) membranes onto PC matrix versus polymerisation time

Figure 4: PPy membranes after PC matrix dissolution a) one polymerisation step, b) three polymerisation steps, c) ten polymerisation steps

Figure 5: SEM micrograph of a cross-section of poly(Py-*co*-PyCOOH) (50:50) membrane : $Ø_{tubes}$ = 1µm; pore length = 18 µm; wall thickness = 240 nm

Figure 6: Typical Taurin low-mass negative ToF-SIMS spectrum

Figure 7: Typical Taurin substituted poly(Py-*co*-PyCOOH) low-mass negative ToF-SIMS spectrum

Figure 8: XPS C_{1S} core level spectra of Taurin substituted (Δ) and non-substituted (●) poly(Py-*co*-PyCOOH) (50:50) –spectra were normalized at 30 scans-

Figure 9: XPS C_{1S} core level spectrum of (a) poly(Py-*co*-PyCOOH) (50:50) -30 scans- and (b) Taurin substituted poly(Py-*co*-PyCOOH) (50:50) -50 scans- : (◇) raw data; (⁻) fit result; (--) base line; (◆) C=C P2VP equivalent; (Δ) C-S; (▲) =C-N; (■) amide; (▼) COOH; (○) shake up

Figure 10: FTIR spectra in transmission mode of (a) poly(Py-*co*-PyCOOH) (50:50) [─] and (b) Taurin substituted poly(Py-*co*-PyCOOH) (50:50) [─]-32 scans-

Figure 11: TG curves of PPy powder (⁻ Δ ⁻), PPy membrane (──),Taurin substituted poly(Py-*co*-PyCOOH) (---), poly(Py-*co*-PyCOOH) (⁻.⁻.⁻)

Poly(PPy-*co*-PPyCOOH)   Poly(PPy-*co*-PPyCONHtaurin)
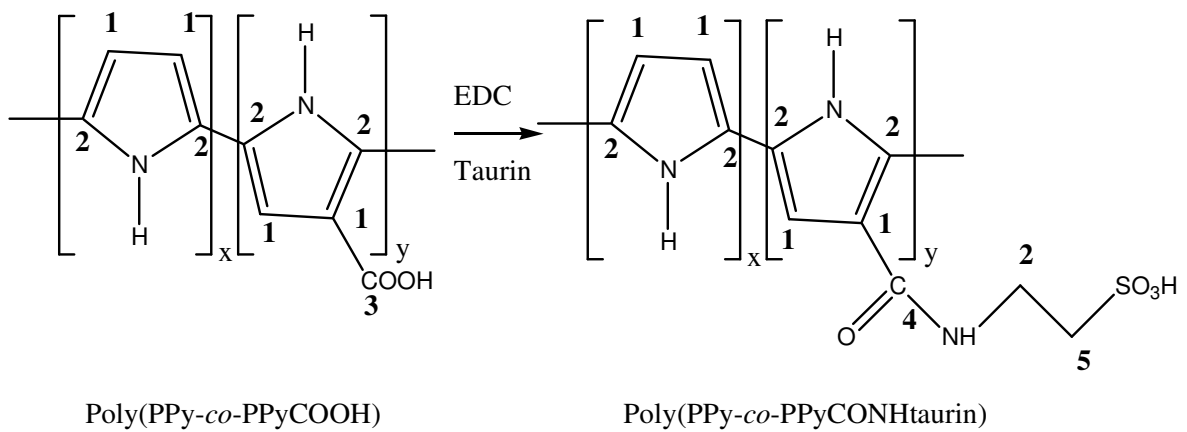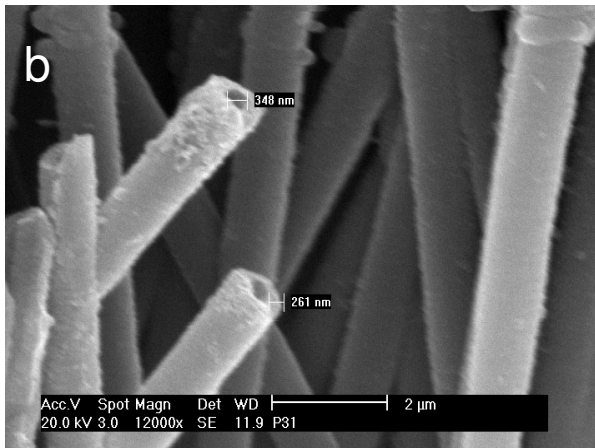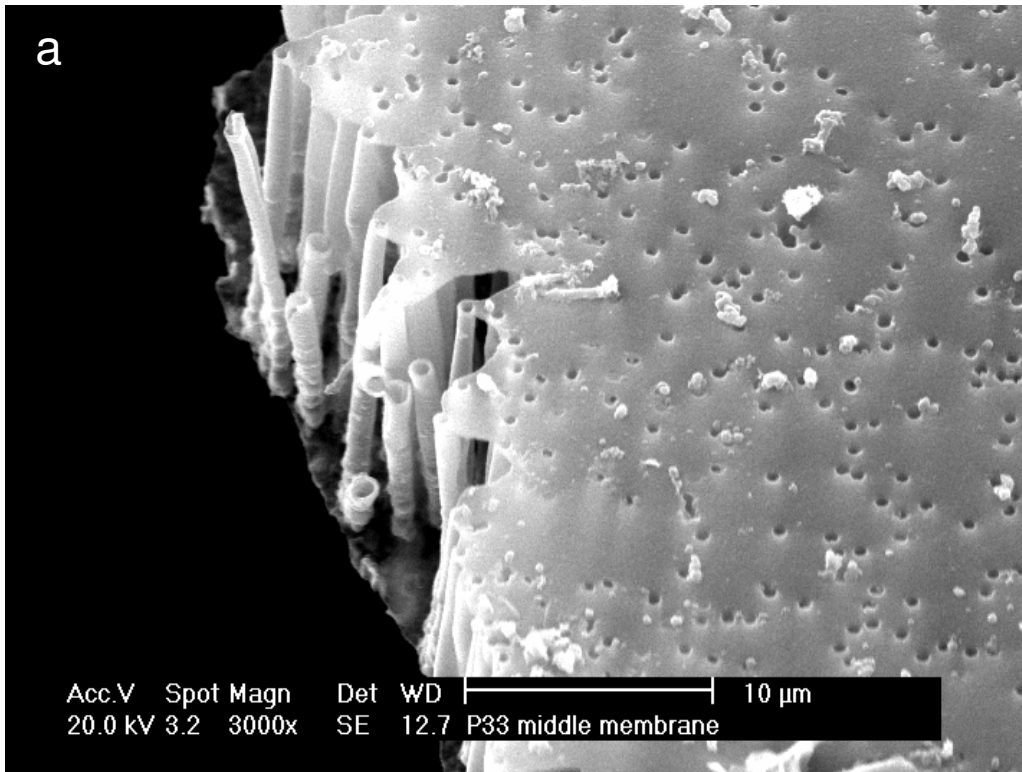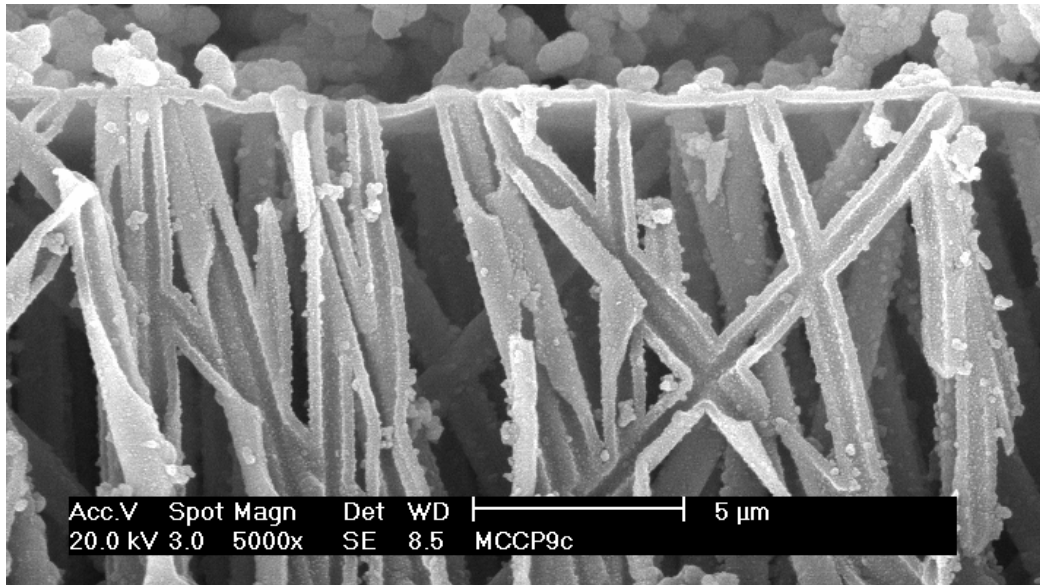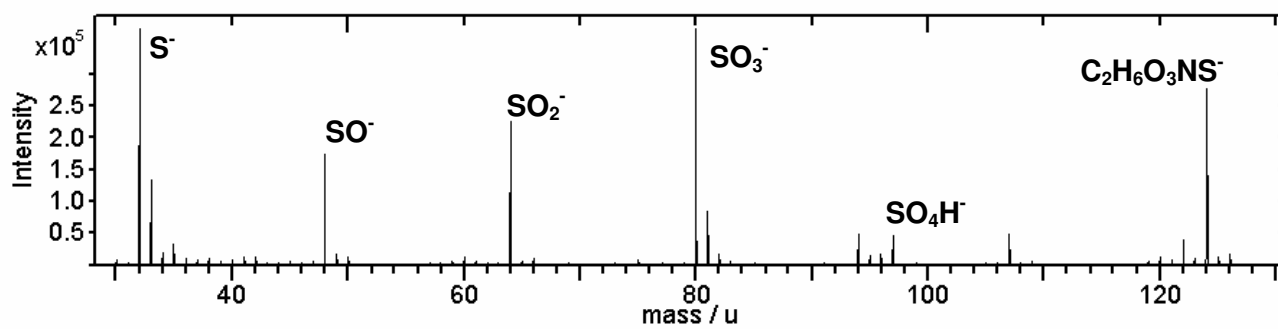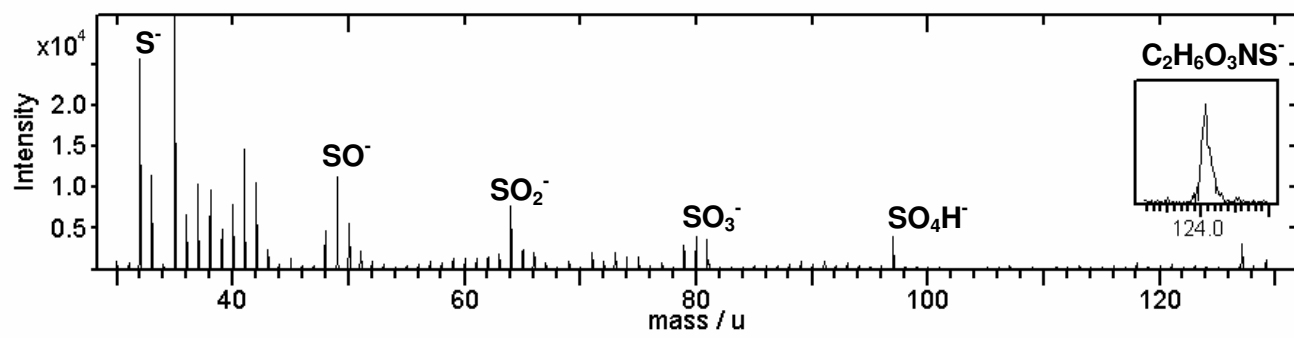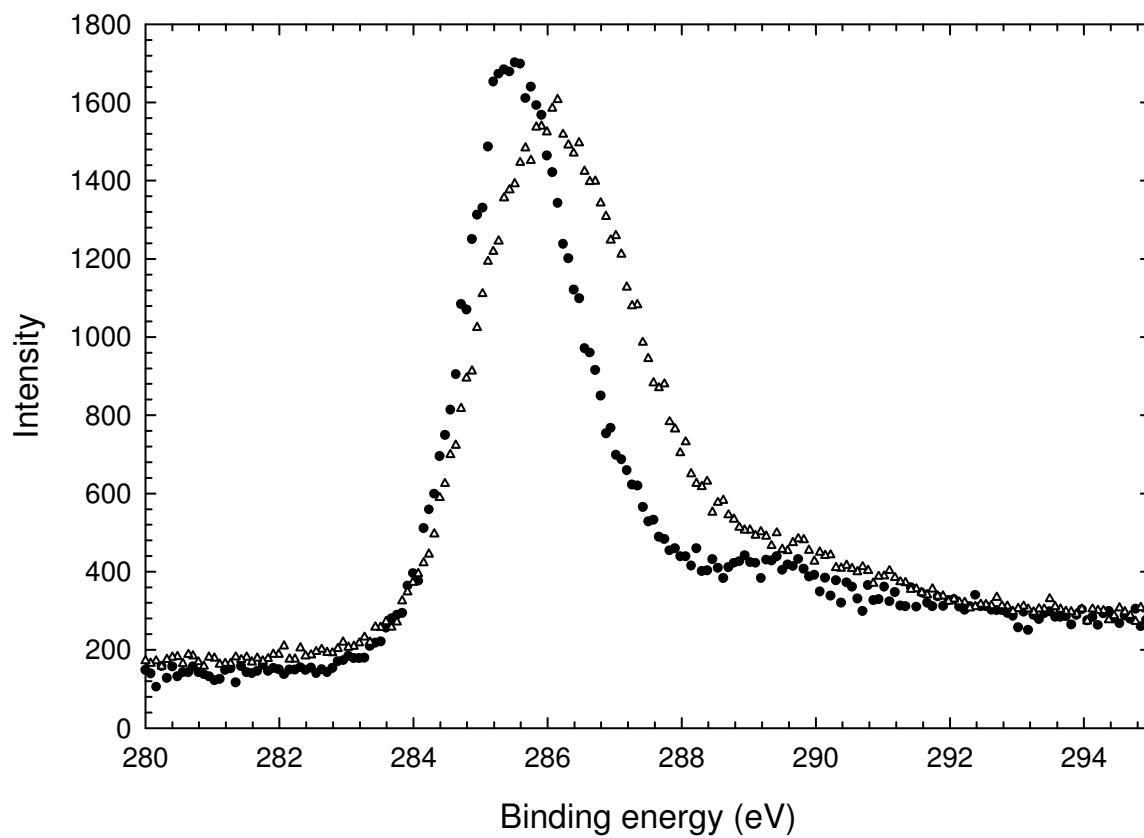
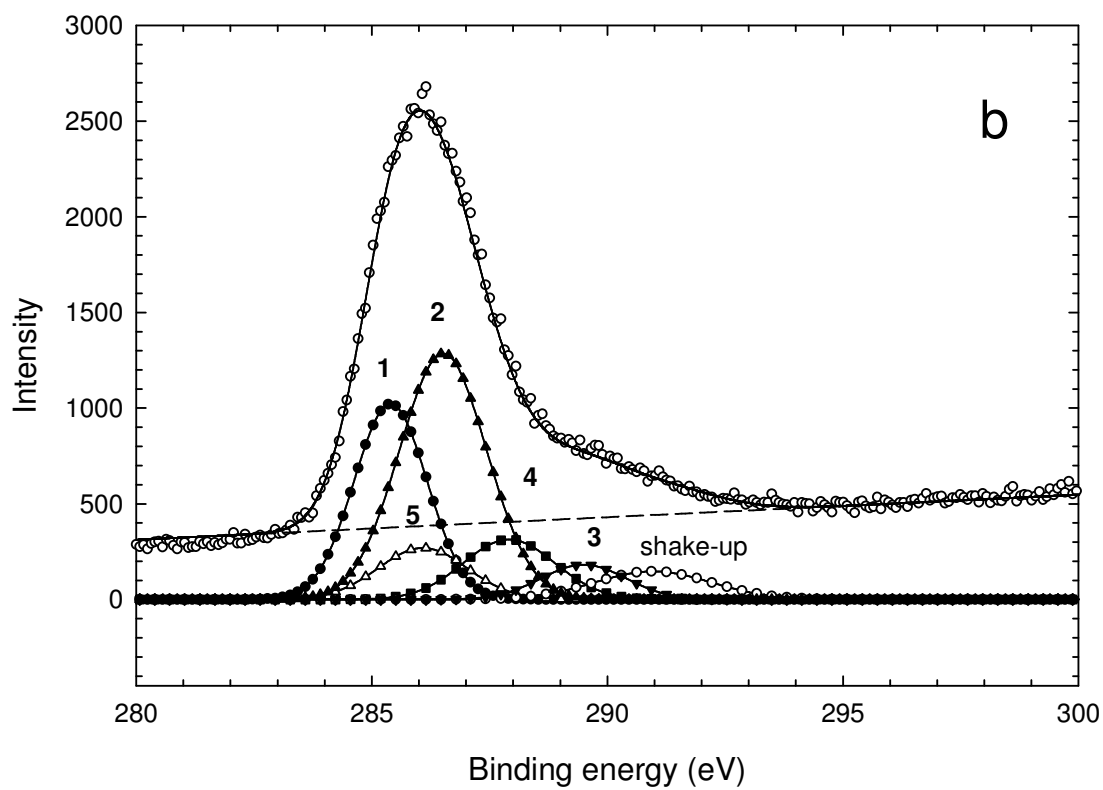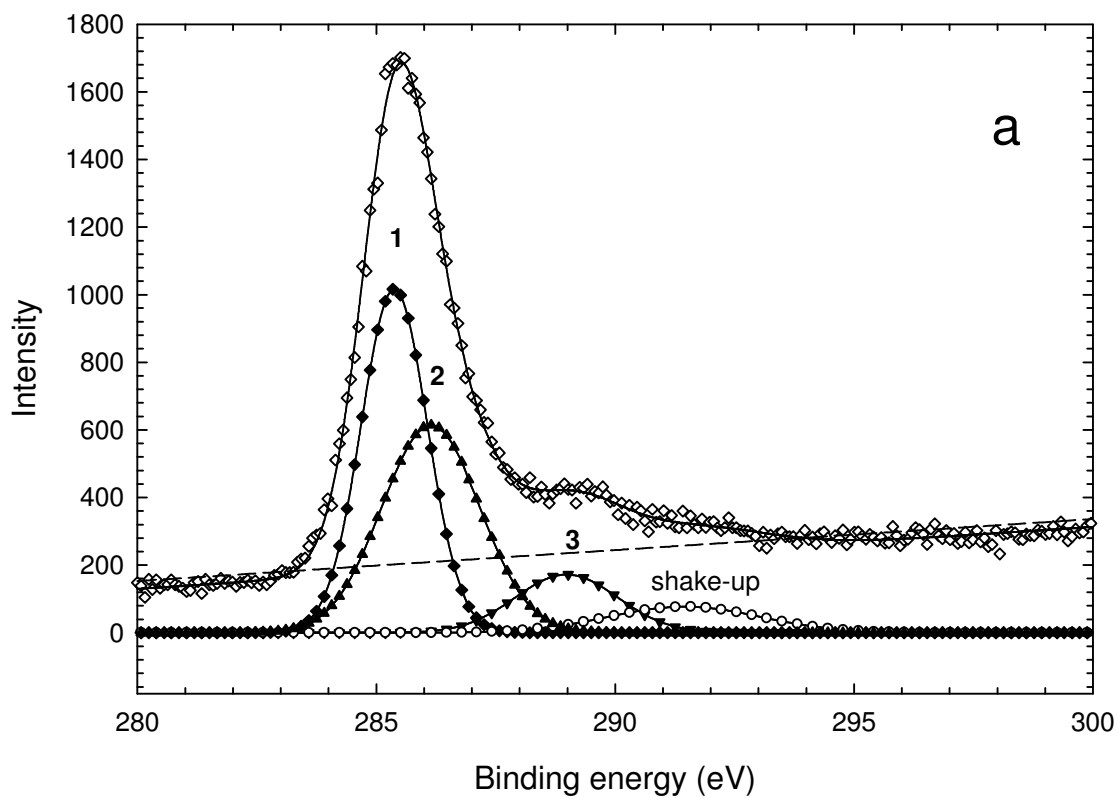Scheme 1
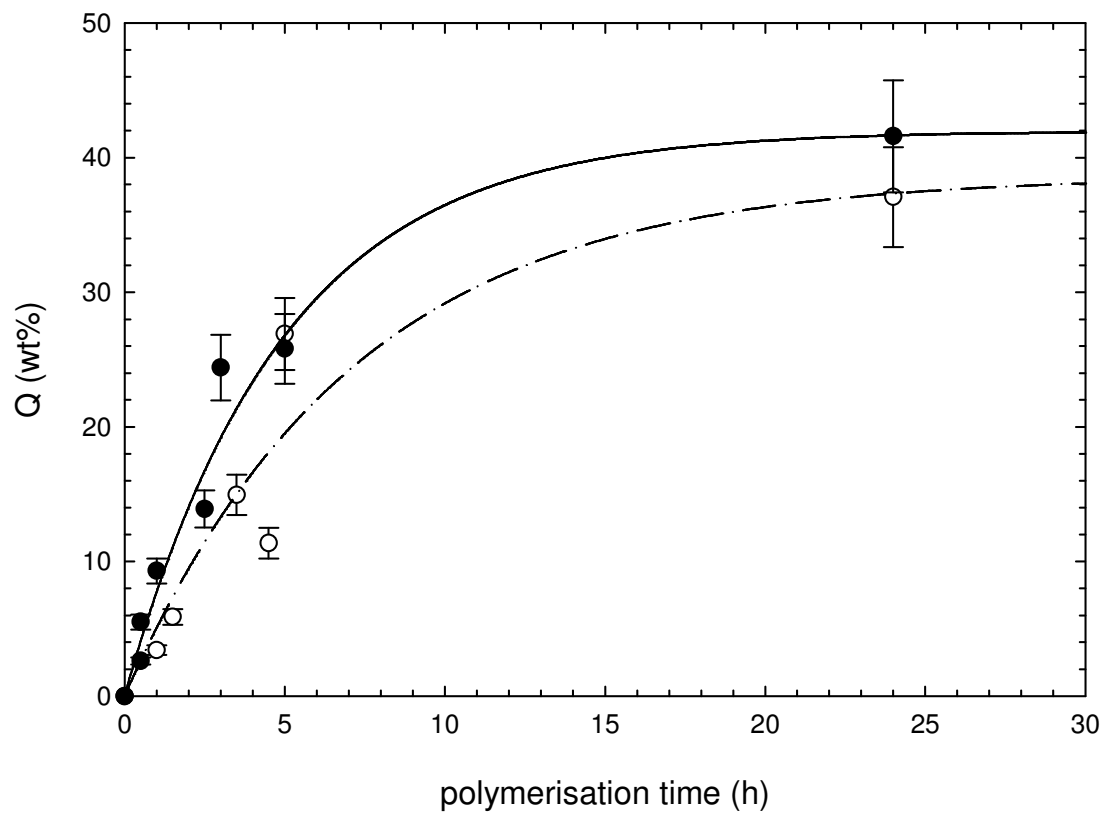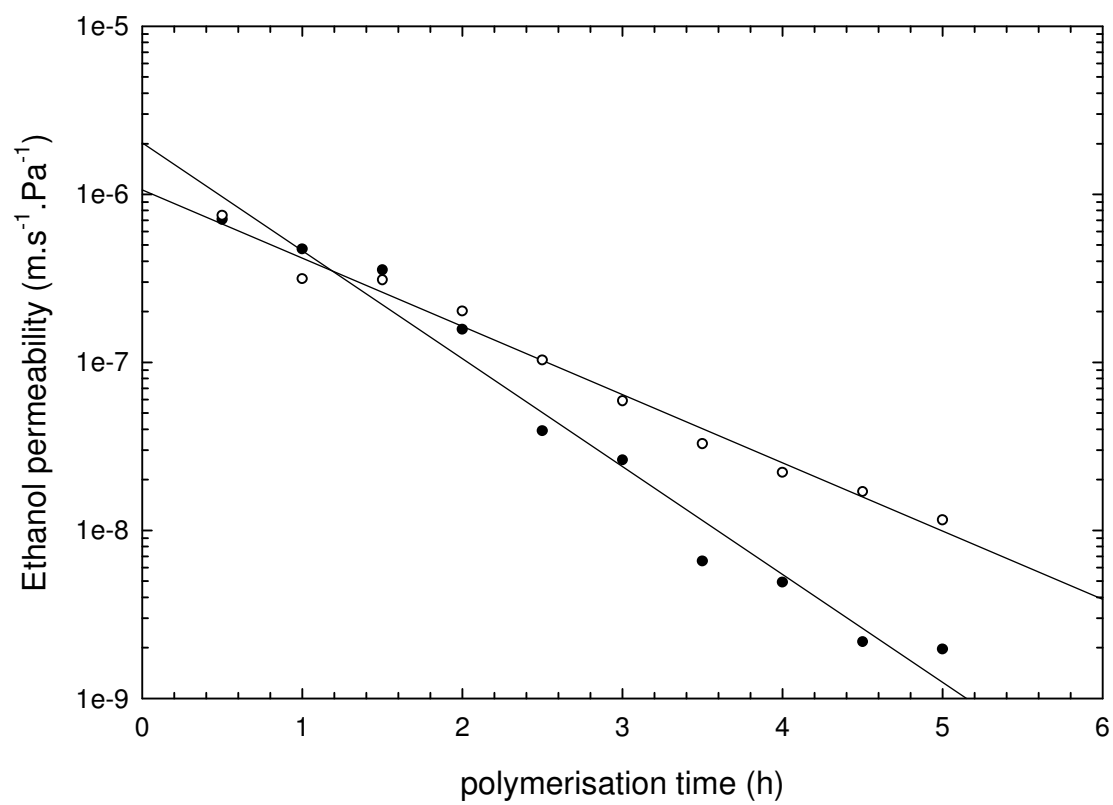
Figure 1

Figure 2
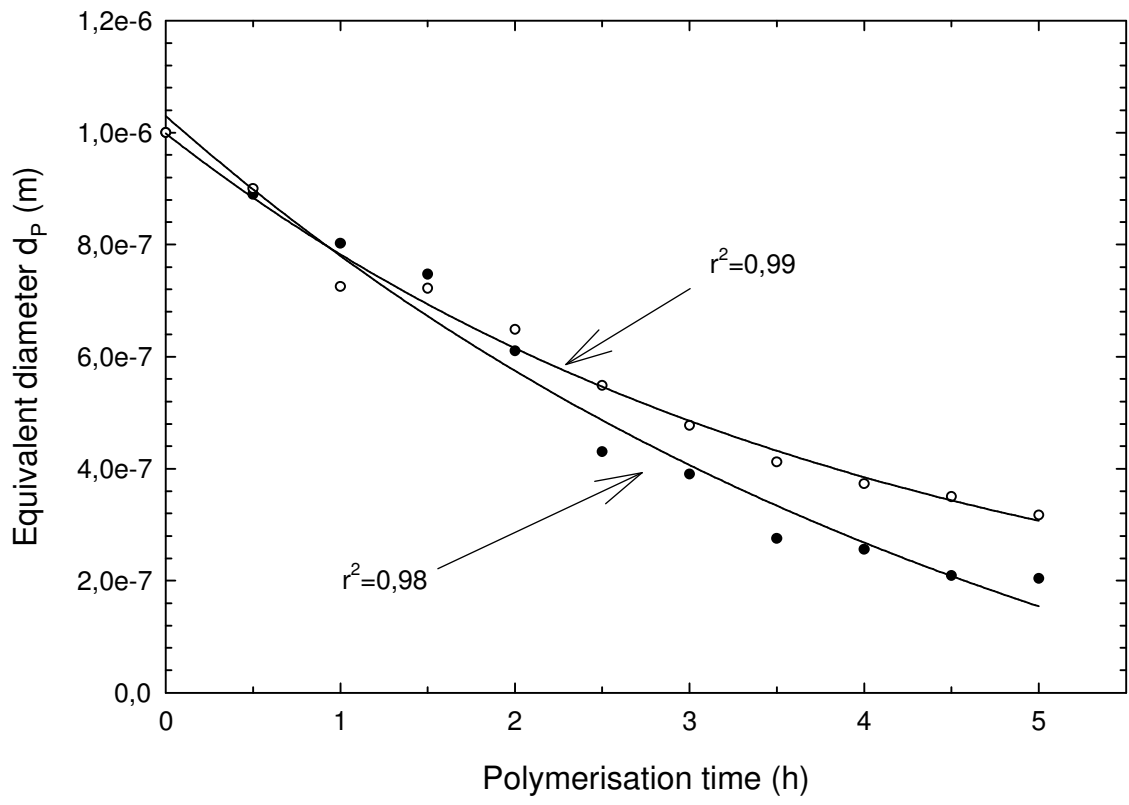
Figure 3
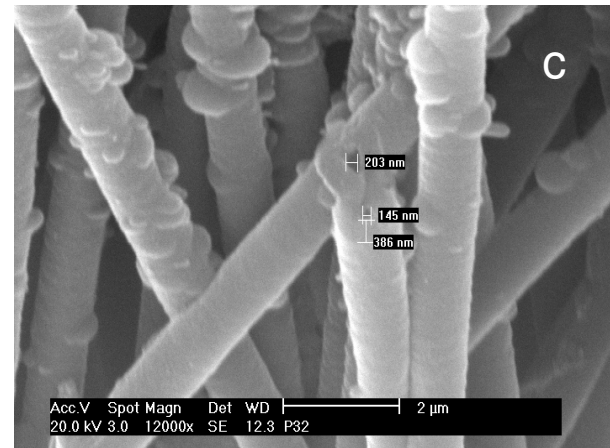
Figure 4

Figure 5

Figure 6

Figure 7

Figure 8

Figure 9

Figure 10

Figure 11